

AD-A145 110

INVESTIGATION OF ICE DYNAMICS IN THE MARGINAL ICE ZONE

1/1

HDL MARINE RESEARCH INST HELSINKI (FINLAND)

M. TEPPEAERANTA ET AL., AUG 84 DAJA45-83-C-0034

UNCLASSIFIED

T/G 8/12

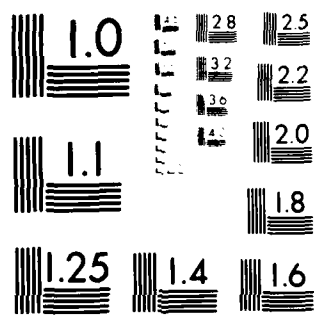
NL

END

DATA
FILED

9-84

DTIC



MICROCOPY RESOLUTION TEST CHART
NATIONAL BUREAU OF STANDARDS

AD-A145 110

DTIC FILE COPY

Unclassified

SECURITY CLASSIFICATION OF THIS PAGE (When Data Entered)

(1C)

REPORT DOCUMENTATION PAGE		READ INSTRUCTIONS BEFORE COMPLETING FORM
1. REPORT NUMBER	2. GOVT ACCESSION NO.	RECIPIENT'S CATALOG NUMBER
	AD-A145 110	
4. TITLE (and Subtitle) Investigation of Ice Dynamics in the Marginal Ice Zone.		5. TYPE OF REPORT & PERIOD COVERED Fourth Interim Report 4 Sep 84 - May 84
7. AUTHOR(s) Dr. Matti Lepparanta		6. PERFORMING ORG. REPORT NUMBER DAJA45-83-C-0034
9. PERFORMING ORGANIZATION NAME AND ADDRESS Institute of Marine Research PO Box 166 Helsinki, Finland.		10. PROGRAM ELEMENT, PROJECT, TASK AREA & WORK UNIT NUMBERS 61102A-IT161102-BH57-01
11. CONTROLLING OFFICE NAME AND ADDRESS USARDSG-UK PO Box 65, FPO NY 09510		12. REPORT DATE Aug 84
		13. NUMBER OF PAGES 23
14. MONITORING AGENCY NAME & ADDRESS(if different from Controlling Office)		15. SECURITY CLASS. (of this report) Unclassified
		15a. DECLASSIFICATION/DOWNGRADING SCHEDULE
16. DISTRIBUTION STATEMENT (of this Report) Approved for public release; distribution unlimited.		
17. DISTRIBUTION STATEMENT (of the abstract entered in Block 20, if different from Report)		
18. SUPPLEMENTARY NOTES AUG 23 1984 <i>[Handwritten signature]</i>		
19. KEY WORDS (Continue on reverse side if necessary and identify by block number) Arctic; pack ice; marginal ice zone; ice dynamics; ice kinematics; ice floes.		
20. ABSTRACT (Continue on reverse side if necessary and identify by block number) The report consists of an initial analysis of the ice kinematics field data from MIZEX-83 Greenland Sea Study. The data set consists of distance measurements accurate to 1-2 metres between Del Norte units at five sites, with one site being the ship. The data set represents a unique set of measurements of the deformation field of a series of interacting floes.		



A-1

INVESTIGATION OF ICE DYNAMICS IN THE MARGINAL ICE ZONE

Principal Investigator: Dr. Matti Leppäranta

Contractor: Institute of Marine Research, Finland

Contract Number: DAJA45-83-C-0034

Fourth Periodic Report

18 September 1983 - 31 May 1984

The research reported in this document has been made possible through the support and sponsorship of the U.S. Government through its European Research Office of the U.S. Army. This report is intended only for the internal management use of the Contractor and the U.S. Government.

APPROVED FOR PUBLIC RELEASE: DISTRIBUTION UNLIMITED

84 08 21 023

FOURTH INTERIM REPORT

Contract No. DAJA45-83-C-0034 (82 Dec 22)

Contractor: Institute of Marine Research, Finland

INVESTIGATION OF ICE DYNAMICS IN THE MARGINAL ICE ZONE

by Dr. Matti Leppäranta (principal investigator) and Dr.
William D. Hibler III (CRREL)

The entitled research work was commenced by the first author on January 24, 1983, at the U.S. Army Cold Regions Research and Engineering Laboratory (CRREL), Hanover, NH, and is done in cooperation with the second author. The work includes both a theoretical and an experimental part. This report considers our initial analysis of the ice kinematics field data from MIZEX-83 Greenland Sea Study. The results have been very useful for planning the MIZEX-84 ice dynamics field measurements. Final analysis will be made using the data of both experiments together. Our basic data set consists of distance measurements accurate to 1-2 m between Del Norte units at five sites with one site being the ship.

The basic configuration of the array is shown in Figure 1 which is drawn to scale for 29 June 08:00 GMT. Each complete Del Norte "measurement" consists of measuring directly the 7 distances d_0 , d_1 , d_2 , d_3 , b_1 , b_2 , b_3 as noted in this figure. These distances are measured to an accuracy of 1-2 m. Other distances are triangulated and will be less accurate with the precise measurement error depending on the geometry of the array. It was initially planned to make measurements every hour or so, but once data began to be acquired it became obvious that shorter time intervals would be necessary to resolve all motion occurring. Accordingly, the acquisition computer was reprogrammed to automatically acquire data at 3 minute intervals. This operational mode was employed throughout the

experiment although there were occasional data gaps due to battery failure, polar bear problems and interference from less accurate Motorola transponders located on certain floes. Such active "ship's radar" transponders will not be necessary in the future as it was found that passive transponders could be effectively located for angular measurements provided their distances were known from the Del Norte units. It should also be noted that the rotation of the array is critical only when one wants to have the north and east components of relative ice drift. The Del Norte system itself gives the strain rate invariants very accurately without the need for any other angular measurements.

While the main measurement program occurred with the ship moored to a floe, data was also taken before and after the center floe deployment with the ship moving. This was made possible by the automated nature of the system which allowed one measurement event to be made in about 15 sec, during which time the ship's motion was relatively small. Triangulation could then be made of the relative positions of points on the ice.

In terms of the overall field operation, there were no major problems and generally the system operated much better than expected. Battery lifetimes were about 4 days, but varied with different types of transponders. The connection system for the batteries will be improved for MIZEX 84 to facilitate easier battery replacement. One minor problem was that the tripod height (about 4 m) was a bit low for the initial baseline unit which was initially at site C. To correct this the baseline tripod was raised about 1.5 m and moved to site D. In addition, after about 5 days one master unit began malfunctioning and had to be replaced. Overall

the automated nature of the system together with its high accuracy proved most valuable. These features allowed the acquisition of by far the most detailed and temporally dense ice deformation measurements in existence to date.

In addition to transponders, sites 0, C and J were equipped with current meter strings moored to toroid buoys. As discussed below the large deformation rates observed demonstrate the necessity of accurate ice deformation measurements in order to precisely interpret the current measurements. Basically, relative ice drift rates of 2 to 3 centimeter per second, and sometimes 8 cm/s, were common. Often these events would last for only a few hours so that fine temporal resolution becomes critical. Because of these large ice motion fluctuations, observed variations in current meter readings may be due to ice motion in many cases.

The ice pack was relatively homogeneous over the region covered by the triangle. Ice floes were typically 30-50 m in diameter and the compactness of ice was 80 to 90 percent. Figure 2 shows a photograph over the ice taken from the helicopter at an altitude of about 5000 ft. To a first approximation the ice pack is an almost ideal two-dimensional granular media, and our measurement scale is good for studying its small scale deformation. The pack was a mixture of first-year and multiyear ice with thickness ranging from one to four meters.

The overall long-term character of the deformation is shown in Figures 3-4. Figure 3 shows the area of the triangle at 1/2 hr intervals over the drift station experiment. The curve has been smoothed with a low pass symmetric filter with 241 weights and a transition band from 48 to 60-

minute periods. The filter design is described in Hibler (1972). Figure 4 shows the triangle configuration at approximately the beginning, middle, and end. Further, Figure 4 shows the approximate relative position and orientation of the ice edge. As can be seen from Figure 3, the area shows a rapid opening and closing early in the experiment followed by a gradual convergence and then a major closing-opening-closing cycle during the last several days of the experiment. Examination of Figure 4 shows this event over the last several days is accompanied by a major shearing of the triangle with the southern points moving northeastward relative to the northern point. This overall convergence is consistent with the light southerly winds during the experiment and the generally northeastward drift which would tend to push the ice edge back into the main pack. Note, however, that there are fluctuations on top of this trend. Also, although not shown there is some indication that the shearing is greater than the convergence as one would expect for a relatively incompressible two-dimensional interacting ice field.

With regard to orientation, the baseline (Polarbjørn - site D) rotated about 20 degrees during the drifting phase (Fig. 5). This caused a relative motion in the array comparable to the strain motion measured with the Del Norte system. Because the accuracy of the orientation angle is only 0.5 degrees, large uncertainties arise when transforming the Del Norte data to a north-east coordinate system. These uncertainties do not, however, affect the strain rate invariants. At the distance of 5 km, a 0.5-degree sector is 40 m wide. Also shown in Figure 5 is the rotation of Polarbjørn measured with gyrocompass. The large bump in the day 184 is man-caused

because of the necessity to change the ship's mooring. The two rotation curves show similar behavior but the high frequency fluctuations are much more pronounced for Polarbjørn.

Table 1 gives the position of the Del Norte sites in north-east coordinates at 6 hr intervals. Their accuracies are $\delta x \approx 0.01 \cdot |y|$, $\delta y \approx 0.01 \cdot |x|$. These large errors are due to the orientation uncertainty discussed above. The baseline orientation is given in Table 2. Note that the direction is counted counterclockwise from east; the numbers thus tell that the direction is slightly southward from west (see also Fig. 1). The data in Table 1 was used to estimate the zeroth and first-order terms of six-hour mean ice velocities using the linear model (see e.g. Hibler et al. 1974)

$$u = u_o + x \cdot \partial_x u|_o + y \cdot \partial_y u|_o + e_u ,$$

$$v = v_o + x \cdot \partial_x v|_o + y \cdot \partial_y v|_o + e_v ,$$

where the subscript o refers to Polarbjørn and (e_u, e_v) is the error term. The results are presented in Table 3. The inaccuracy due to measurement error is 0.1 cm/s for the constant terms u_o and v_o and $0.1\% h^{-1}$ for the first-order derivatives. Also are shown the principal strain rates (E1 and E2), the direction of the first principal axis (AE1), divergence (EI), twice the maximum shear rate (EII) and vorticity (VOR). The goodness of fit, defined as the ratio of the explained variance to the total variance, (last column) is typically 85-95%.

Analysis of finer time scale data shows there are a large variety of significant fluctuations superimposed on the overall trends. This is

illustrated in Figures 6 and 7 which show raw and filtered distances at 3-minute intervals. As can be seen the filtered record shows large variations on time scales of a few hours. In the raw data, there are significant fluctuations over half hour intervals. These fluctuations are undoubtedly related to floe bumping as well as randomness in the forcing fields. However, it is also possible that they are due to more organized floe interactions which can manifest themselves as kinematic waves propagating across the array. Numerical studies by Hibler et al. (1983) have shown such waves and fluctuating effects in time can arise in a nonlinear plastic sea ice model even though the external forcing is temporally constant. The simplest example of such a wave is a "ridging front" that can occur, for example, if one pushes in one end of a series of equally separated floes (or billiard balls) and watches the collisions propagate through in a like manner to a chain reaction auto collision. A possible example of such an event is at about 20:00 GMT on July 7 (Julian day 188) in lines d_0 and d_3 . Note the sudden reversal of distance in d_0 at this time after convergence had been occurring for some time in the line d_3 . In addition to this simple ridging front, simulations have shown more complex propagating wave effects can arise if the coupling between the ice strength and compactness is nonlinear.

An interesting feature in the recordings was the presence of occasional sudden slips of the order of tens of meters. These effects probably arise due to an overshooting phenomenon in the ice stress which causes the distance to change rapidly and then remain approximately at a constant level. An example is shown in Figure 8 where a time series of the

distance d_0 has been drawn. In the days 181 and 182 four such slips occurred.

A perhaps more illustrative example of fluctuations is shown in Figure 9 which show the relative velocities between the ship (moored to a floe) and stations O and J. These have been obtained through first central differencing the raw data and then filtering with a low pass symmetric filter with 241 weights and transition band from 48 to 60-minute periods (Hibler, 1972). The relative velocities are very large with fluctuations up to 8 cm/s occurring. Since variations in the ice motion will also affect current water strings attached to ice floes, these results emphasize the necessity of making detailed ice motion measurements to properly interpret current measurements made from ice.

The stretch speed (i.e. rate of change of distance) between Polarbjørn and the sites on ice was obtained very accurately with the Del Norte system. Figure 10 shows the spectra of the stretch speeds up to the frequency of 24 cycles per day. The measurement noise lies below the lowest indicated spectral density value. For the sites O and J, there is a peak close to 2 cycles per day. In the higher frequencies the spectral density falls off with a red noise character. A comparison with the radar observations (Fig. 11) shows that the radar also gives the peak at about 2 cycles per day but then the spectral density falls off much more rapidly than in the case of Del Norte data. Part of this fall off is due to linear interpolation between 2 hr interval radar measurements during parts of the experiment. This large sampling interval was used because the distance changes were too small to be resolved by the radar. Due to its inaccuracy

it is unlikely that the radar can resolve higher frequencies than about three cycles per day, unless deformation rates are substantially larger than observed here, (which likely will occur closer to the ice margin).

Overall this data set represents a unique set of measurements of the deformation field of a series of interacting floes floating in the ocean. Because of the fine temporal resolution, accuracy of the measurements, and coincidence of current and wind measurements, this data should greatly aid in sorting out the physics of marginal ice zone ice dynamics and kinematics. Such efforts are currently in progress.

References

Hibler, W.D., III, 1972: Design and maximum error estimation for small error low pass filters. CRREL Research Report 304.

Hibler, W.D., III, W.F. Weeks, A. Kovacs and S.F. Ackley, 1974: Differential sea-ice drift. I. Spatial and temporal variations in sea ice deformation, J. Glaciology, 13, 437-455.

Hibler, W.D., III, I. Udin and A. Ullerstig, 1983: On forecasting mesoscale ice dynamics and buildup. Annals of Glaciology, vol. 4, 110-115.

Figure Captions

1. Configuration of strain array and nomenclature for distances discussed later in the paper. The triangle is plotted to scale for 29 June 08 GMT, and the ship (Polarbjørn) is located at the center point P and was moored to an ice floe. Del Norte units are located at circled points. Directly measured distances (accurate to 1-2 m) are denoted by subscripted b's and d's while distances calculated by triangulation (less accurate depending on geometry) are denoted by subscripted s's.
2. Photograph of ice floes near the center of the strain array. The location of the Polarbjørn is noted, which for scale is 50 m long. This photograph was taken by Dr. Vernon Squire of the Scott Polar Research Institute as part of an aerial survey carried out by helicopter flights.
3. The area of the triangle OCJ at 1/2 hr intervals filtered with a low pass filter with transition band from 48 to 60-minute periods. The high frequency variations during Julian days 184.5 to 186.5 are due to problems with the measurement system (a poorly functioning master unit).
4. Configuration change of the triangle over the period of the experiment. Also shown is the approximate location and orientation of the ice edge drawn to scale.
5. Orientation of the baseline (line from the ship to the site D) and the heading of Polarbjørn at one-hour intervals over period of the experiment. The angle increases counterclockwise, and the zero points east.
6. Raw measured distances during a 12 hr period in the early part of the experiment. The vertical scale shows the distance scale and absolute initial values are listed for each curve.
7. Distances filtered with a low pass filter (transition band 48 to 60-minute periods) during a 30 hour period in the late part of the experiment. The vertical scale shows the distance scale and absolute initial values are listed for each curve.
8. Illustration of slips in the distance d_0 (raw data).
9. Rate of change of the distances d_1 and d_3 during 30 hours in late part of the experiment. The time series has been filtered with a low pass filter (transition band 48 to 60-minute periods).
10. The spectra of the rate of change of the distances d_1 , d_2 and d_3 .
11. The spectra of the rate of change of the distance d_1 as measured with the Del Norte system and by using the ship's radar.

Table 1.

M I Z E X - 8 3 / G R E E N L A N D S E A

POSITIONS OF THE DEL NORTE STATIONS WITH RESPECT TO POLARBJORN IN NORTH-EAST COORDINATE SYSTEM. TIME IS GMT. X AND Y ARE IN KILOMETERS.

STATION:			BILL (D)		OLA (O)		CYCLESONDE (C)		JAMIE (J)	
MO	DAY	HRS	X	Y	X	Y	X	Y	X	Y
6	28	1800	-1.704	-0.153	-2.701	-4.586	-2.164	5.237	4.790	-0.584
6	29	000	-1.616	-0.213	-3.124	-3.957	-2.217	4.645	5.417	0.661
6	29	600	-1.702	-0.439	-3.206	-4.110	-2.894	3.982	4.816	-0.511
6	29	1200	-1.655	-0.473	-3.105	-4.212	-2.835	3.953	4.682	-0.405
6	29	1800	-1.676	-0.508	-3.046	-4.216	-3.139	3.766	4.820	-0.337
6	30	000	-1.717	-0.408	-3.126	-3.956	-3.364	3.735	4.884	-0.883
6	30	600	-1.714	-0.389	-3.121	-3.932	-3.329	3.777	4.848	-0.968
6	30	1200	-1.674	-0.386	-3.100	-3.962	-2.997	3.857	4.727	-0.834
6	30	1800	-1.683	-0.338	-3.051	-3.866	-3.229	3.936	4.783	-1.054
7	1	000	-1.673	-0.350	-3.091	-3.874	-3.096	3.907	4.743	-0.955
7	1	600	-1.653	-0.317	-3.148	-3.846	-3.006	3.992	4.607	-1.101
7	1	1200	-1.626	-0.306	-3.145	-3.840	-2.882	4.059	4.590	-1.098
7	1	1800	-1.631	-0.294	-3.204	-3.803	-2.876	4.106	4.399	-1.490
7	2	000	-1.631	-0.322	-3.047	-3.887	-3.016	4.123	4.483	-1.232
7	2	600	-1.638	-0.304	-3.108	-3.820	-2.932	4.097	4.527	-1.172
7	2	1200	-1.628	-0.305	-3.104	-3.825	-2.907	4.105	4.492	-1.163
7	2	1800	-1.637	-0.281	-2.985	-3.823	-3.076	4.087	4.419	-1.747
7	3	000	-1.628	-0.336	-2.887	-3.903	-3.128	3.999	4.484	-1.455
7	3	600	-1.655	-0.292	-2.986	-3.805	-3.071	4.022	4.554	-1.483
7	3	1200	-1.649	-0.287	-2.974	-3.804	-3.095	4.018	4.473	-1.638
7	3	1800	-1.679	-0.279	-2.929	-3.791	-3.218	4.048	4.555	-1.746
7	4	000	-1.663	-0.315	-2.911	-3.831	-3.198	3.965	4.418	-1.967
7	4	600	-1.688	-0.314	-2.984	-3.814	-3.153	3.904	4.400	-1.840
7	4	1200	-1.664	-0.396	-3.057	-3.914	-3.175	3.788	4.240	-1.632
7	4	1800	-1.654	-0.335	-3.211	-3.837	-3.016	3.919	4.199	-1.586
7	5	000	-1.638	-0.463	-2.975	-4.085	-3.178	3.685	4.184	-1.541
7	5	600	-1.650	-0.432	-3.239	-3.931	-3.091	3.696	4.048	-1.891
7	5	1200	-1.655	-0.386	-2.936	-4.041	-3.129	3.755	4.115	-1.846
7	5	1800	-1.595	-0.475	-2.675	-4.163	-3.459	3.632	4.318	-1.186
7	6	000	-1.572	-0.521	-2.431	-4.224	-3.725	3.474	4.448	-0.993
7	6	600	-1.576	-0.545	-2.367	-4.256	-3.800	3.375	5.283	-1.005
7	6	1200	-1.671	-0.476	-2.325	-3.879	-4.152	3.361	5.276	-1.407
7	6	1800	-1.715	-0.626	-2.208	-3.947	-4.306	2.966	5.507	-1.683
7	7	000	-1.683	-0.641	-2.149	-3.959	-4.300	2.900	5.393	-1.508
7	7	600	-1.713	-0.742	-2.075	-3.975	-4.458	2.666	5.817	-1.484
7	7	1200	-1.694	-0.808	-2.054	-4.034	-4.442	2.529	5.925	-1.097
7	7	1800	-1.686	-0.647	-2.084	-3.773	-4.653	2.787	5.872	-1.738
7	8	000	-1.598	-0.548	-2.267	-3.798	-5.094	3.142	5.329	-2.074
7	8	600	-1.443	-0.389	-1.996	-3.420	-5.210	3.180	5.365	-1.907

Table 2.
M I Z E X - 8 3 / G R E E N L A N D S E A

ORIENTATION OF THE BASELINE IN NORTH-EAST COORDINATE SYSTEM. THE ANGLE IS
COUNTED COUNTERCLOCKWISE FROM THE EAST DIRECTION.

MO	DAY	HRS	ANGLE
6	28	1200	189.9
6	28	1800	185.1
6	29	000	187.4
6	29	600	194.5
6	29	1200	195.9
6	29	1800	196.9
6	30	000	193.4
6	30	600	192.8
6	30	1200	193.0
6	30	1800	191.4
7	1	000	191.8
7	1	600	190.9
7	1	1200	190.7
7	1	1800	190.2
7	2	000	191.2
7	2	600	190.5
7	2	1200	190.6
7	2	1800	189.8
7	3	000	191.7
7	3	600	190.1
7	3	1200	189.9
7	3	1800	189.4
7	4	000	190.7
7	4	600	190.5
7	4	1200	193.5
7	4	1800	191.4
7	5	000	195.8
7	5	600	194.6
7	5	1200	193.1
7	5	1800	196.6
7	6	000	198.2
7	6	600	199.1
7	6	1200	196.3
7	6	1800	200.1
7	7	000	200.7
7	7	600	203.4
7	7	1200	205.4
7	7	1800	200.6
7	8	000	199.4
7	8	600	195.1

Table 3.
MIZEX-83 / GREENLAND SEA

LINEAR FIRST ORDER FIT FOR THE DEL NORTE DATA (SIX-HOUR DISPLACEMENTS) IN NORTH-EAST COORDINATE SYSTEM. TIME IS GMT.

MD DAY HRS	DOU CM/S	DUU Z/H	DYU Z/H	DOV CM/S	DVU Z/H	DYV Z/H	EI Z/H	EII Z/H	EI Z/H	E2 Z/H	AEL DEG	VOR D/H	FIT %
6 29 0	0.41	1.90	0.50	1.38	2.64	-2.20	-0.30	5.16	2.43	-2.73	57.2	0.61	91.8
6 29 600	-1.31	-0.49	-1.19	-2.13	-1.58	-0.93	-1.42	2.81	0.69	-2.11	-26.6	-0.11	64.7
6 29 1200	-0.01	-0.46	-0.07	0.01	0.37	0.14	-0.32	0.66	0.17	-0.49	48.8	0.13	99.9
6 29 1800	-0.08	0.53	-0.76	-0.12	0.34	-0.38	0.14	1.00	0.57	-0.43	-69.9	0.32	98.0
6 30 0	-0.21	0.44	-0.30	-0.48	-1.40	-0.62	-0.17	2.00	0.91	-1.09	-47.1	-0.32	93.7
6 30 600	-0.01	-0.11	0.06	-0.04	-0.24	0.03	-0.07	0.22	0.08	-0.15	-40.8	-0.09	98.5
6 30 1200	0.21	-0.53	0.65	0.24	0.25	0.23	-0.30	1.18	0.44	-0.74	44.5	-0.12	91.4
6 30 1800	-0.13	0.25	-0.60	-0.11	-0.66	-0.02	0.22	1.29	0.76	-0.53	-50.2	-0.02	97.0
7 1 0	0.06	-0.13	0.36	0.09	0.24	-0.04	-0.17	0.61	0.22	-0.39	35.9	-0.04	96.6
7 1 600	-0.10	-0.29	0.32	-0.06	-0.42	0.12	-0.17	0.43	0.13	-0.30	-69.1	-0.21	96.8
7 1 1200	0.12	-0.14	0.25	0.08	-0.05	0.13	-0.01	0.33	0.16	-0.17	58.0	-0.09	89.0
7 1 1800	-0.28	-0.34	0.16	-0.43	-0.93	0.07	-0.27	0.87	0.30	-0.57	-38.1	-0.31	88.5
7 2 0	0.05	0.04	-0.63	0.29	0.69	0.17	0.21	0.14	0.17	0.03	80.9	0.38	93.7
7 2 600	0.10	0.13	0.30	0.10	0.05	-0.20	-0.07	0.47	0.20	-0.27	49.2	-0.07	90.9
7 2 1200	-0.01	-0.10	0.05	0.02	0.02	0.03	-0.08	0.15	0.03	-0.11	45.7	-0.01	97.6
7 2 1800	-0.20	-0.20	-0.59	-0.75	-1.27	0.02	-0.19	1.88	0.85	-1.03	-42.2	-0.20	84.3
7 3 0	0.08	0.01	-0.32	0.21	0.83	-0.02	-0.01	0.51	0.25	-0.26	44.7	0.33	95.9
7 3 600	0.08	0.27	0.33	0.07	-0.24	-0.17	0.10	0.45	0.28	-0.18	80.0	-0.16	96.5
7 3 1200	-0.12	-0.18	-0.07	-0.20	-0.34	-0.00	-0.18	0.45	0.13	-0.31	-32.7	-0.08	81.9
7 3 1800	-0.02	0.19	-0.35	-0.10	-0.27	0.04	0.23	0.65	0.44	-0.21	-54.5	0.02	97.7
7 4 0	-0.14	-0.34	0.00	-0.42	-0.35	-0.07	-0.41	0.44	0.01	-0.43	-4.6	-0.10	69.9
7 4 600	-0.02	0.07	0.26	0.11	0.28	-0.17	-0.10	0.58	0.24	-0.34	42.1	0.01	96.7
7 4 1200	-0.24	-0.23	0.13	0.05	0.71	-0.02	-0.26	0.86	0.30	-0.56	35.9	0.17	88.5
7 4 1800	0.06	0.03	0.67	0.28	-0.13	0.09	0.12	0.55	0.34	-0.21	50.9	-0.23	90.3
7 5 0	-0.08	-0.29	-0.84	-0.38	0.68	0.04	-0.25	0.37	0.06	-0.31	-36.5	0.43	92.5
7 5 600	-0.19	0.02	0.77	-0.39	-1.02	-0.30	-0.28	0.41	0.07	-0.34	-27.5	-0.51	91.9
7 5 1200	0.13	-0.31	-0.76	0.13	0.22	0.35	0.04	0.85	0.45	-0.41	-59.0	0.28	84.2
7 5 1800	0.05	0.23	-1.26	0.66	1.80	-0.03	0.20	0.59	0.40	-0.20	56.0	0.88	94.2
7 6 0	0.02	0.18	-1.07	0.04	0.66	-0.14	0.04	0.53	0.28	-0.24	-53.7	0.50	99.9
7 6 600	1.08	1.82	-0.08	-0.15	0.11	-0.11	1.70	1.93	1.82	-0.12	89.5	0.05	84.0
7 6 1200	-0.45	0.26	-0.78	-0.28	-1.22	-1.06	-0.80	2.39	0.79	-1.59	-38.5	-0.13	95.7
7 6 1800	0.14	0.43	-0.53	-0.94	-0.15	-0.70	-0.27	1.32	0.52	-0.79	-57.2	0.11	66.4
7 7 0	-0.10	-0.31	-0.21	0.13	0.40	-0.03	-0.34	0.34	0.00	-0.34	0.8	0.17	95.5
7 7 600	0.36	0.86	-0.35	-0.33	0.27	-0.40	0.46	1.26	0.86	-0.40	-87.3	0.18	92.3
7 7 1200	0.18	0.16	0.02	0.25	0.90	0.08	0.24	0.92	0.58	-0.34	51.8	0.25	95.6
7 7 1800	-0.33	0.09	-0.38	-0.28	-1.66	-0.57	-0.48	2.14	0.83	-1.31	-39.2	-0.37	96.1
7 8 0	-1.20	-0.56	-0.66	0.09	-0.83	0.63	0.07	1.90	0.99	-0.92	-52.9	-0.05	57.0
7 8 600	0.07	-0.31	-1.05	0.44	-0.31	-1.02	-1.32	1.53	0.11	-1.43	-8.9	0.21	88.5

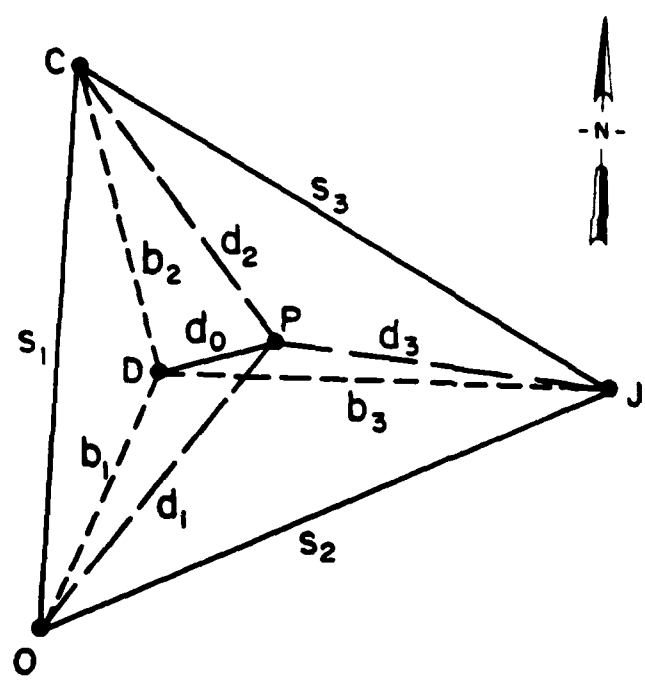
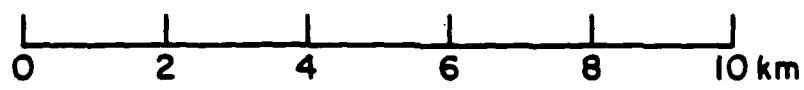
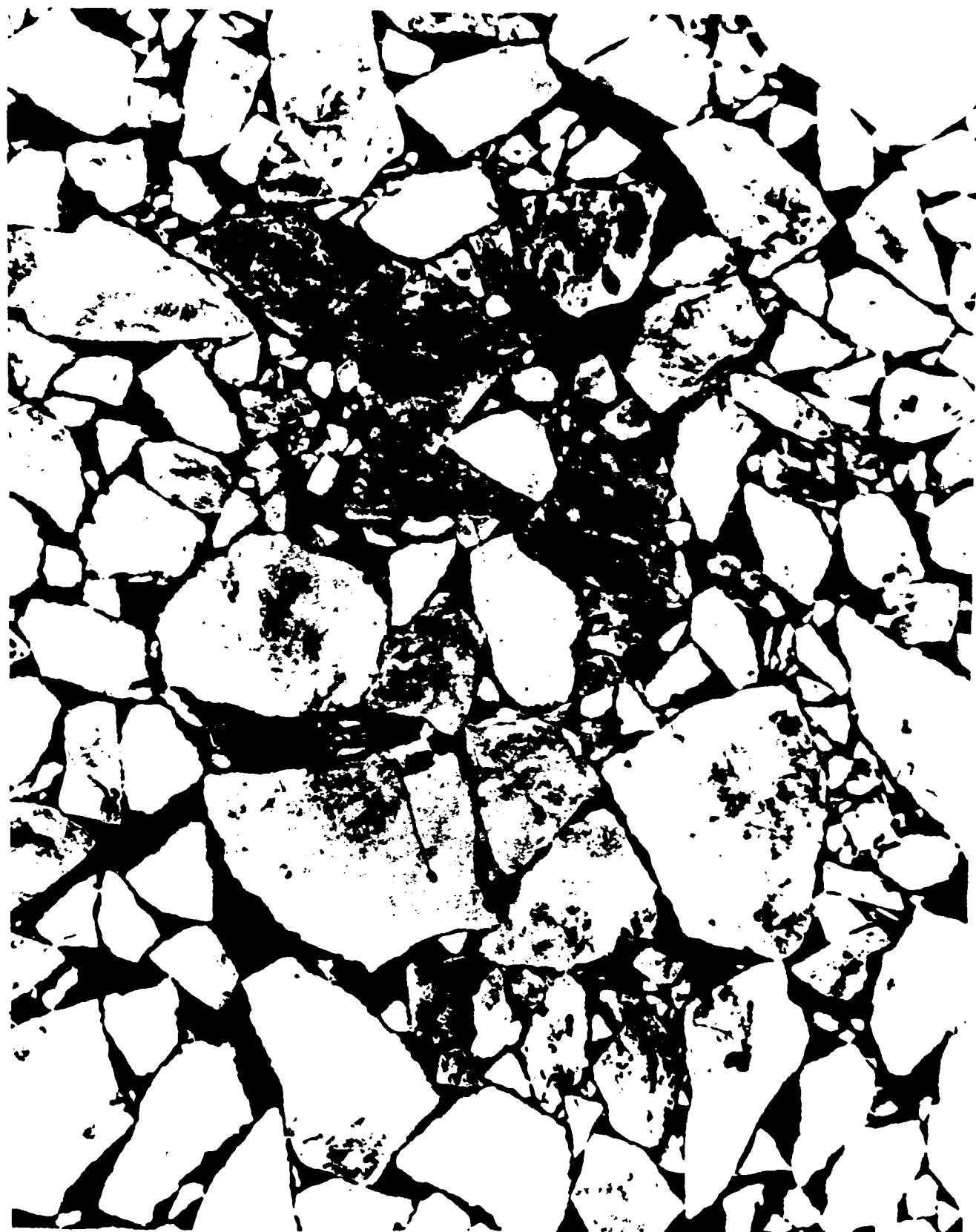
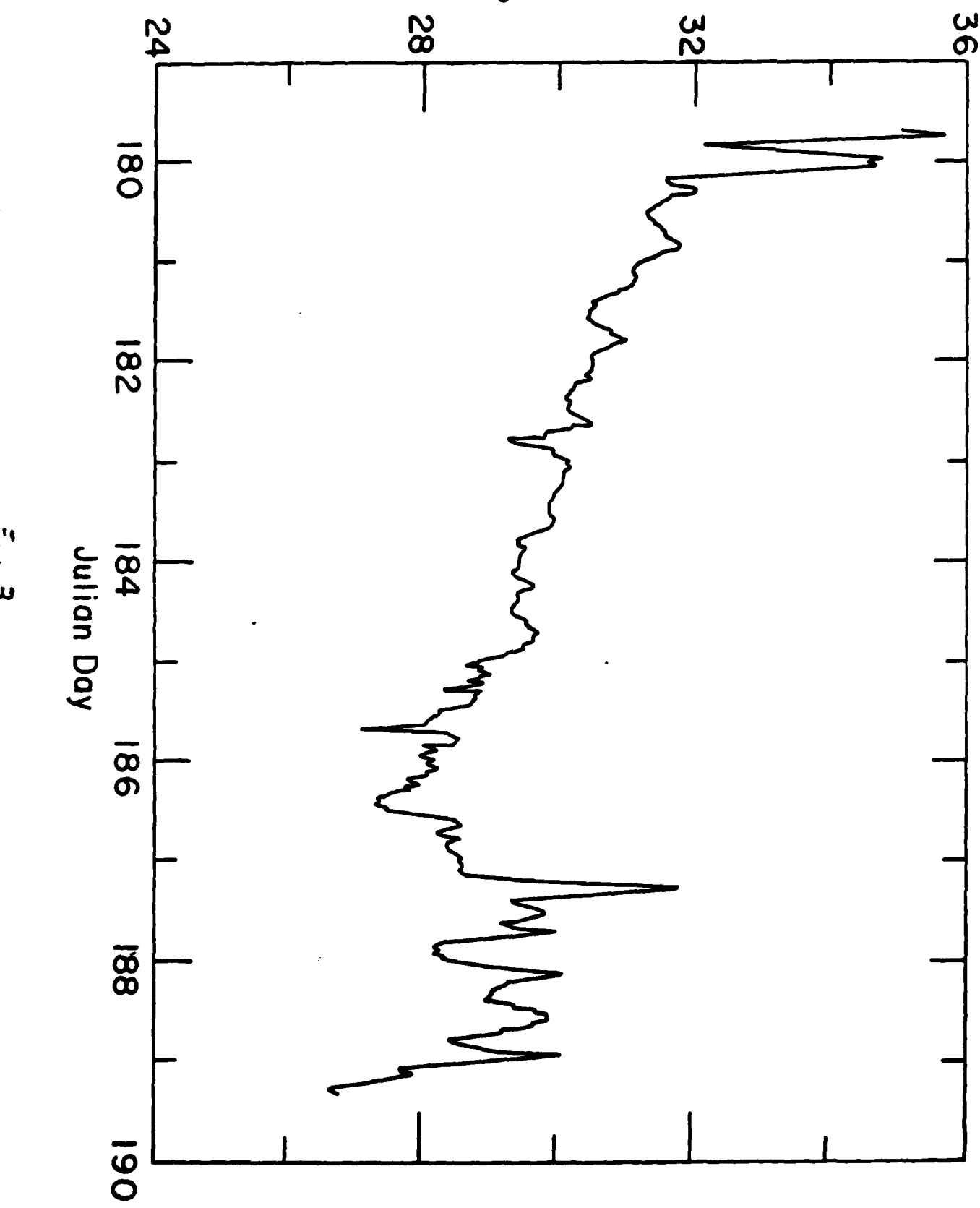


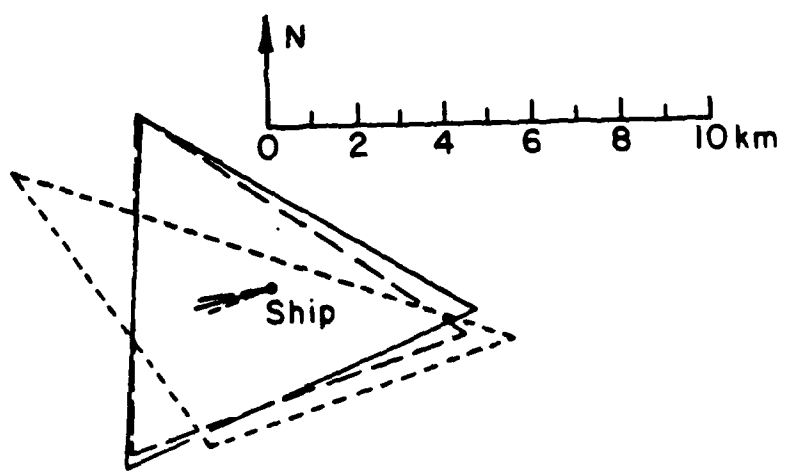
Fig 1



F . 2

Triangle Area (km^2)

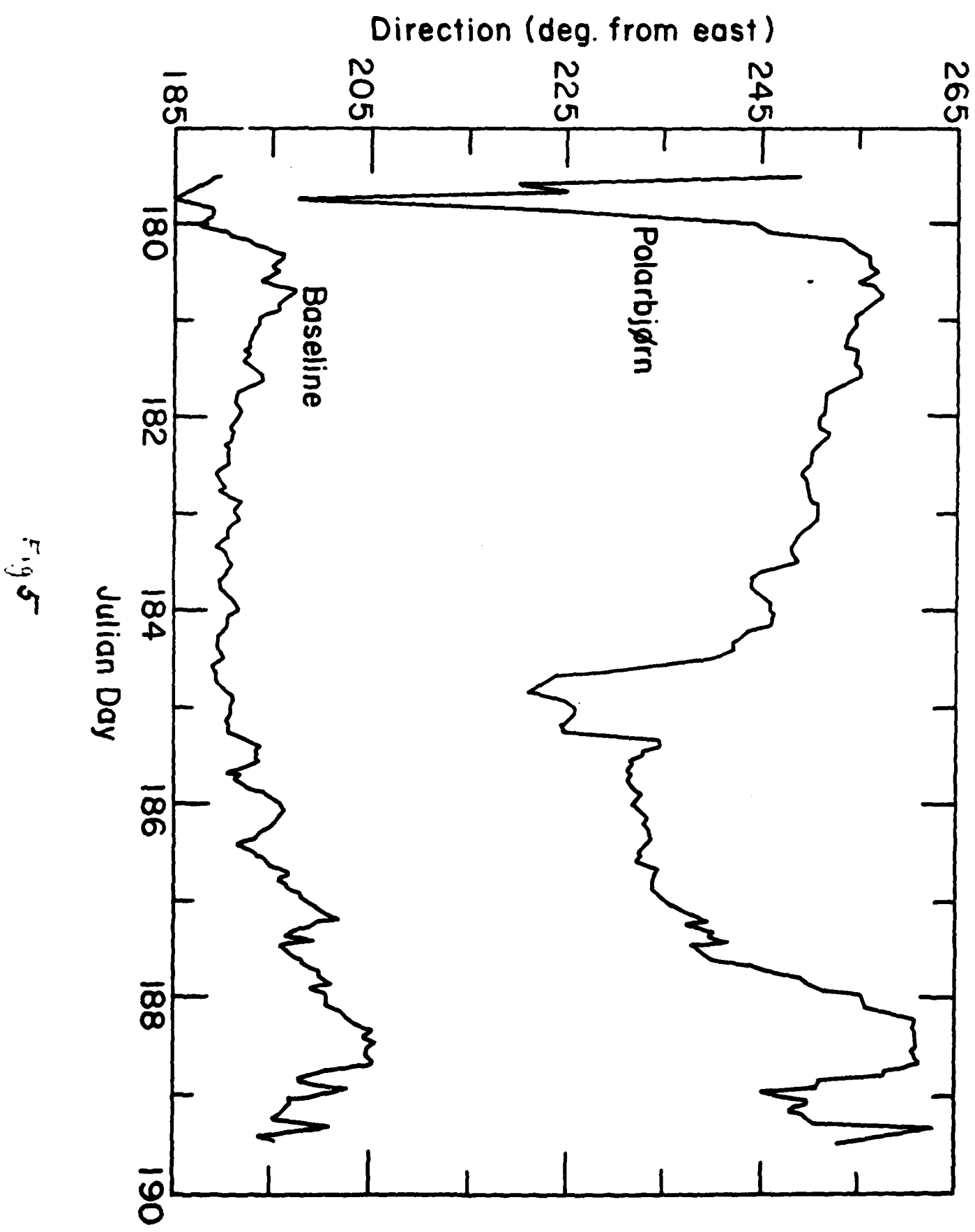


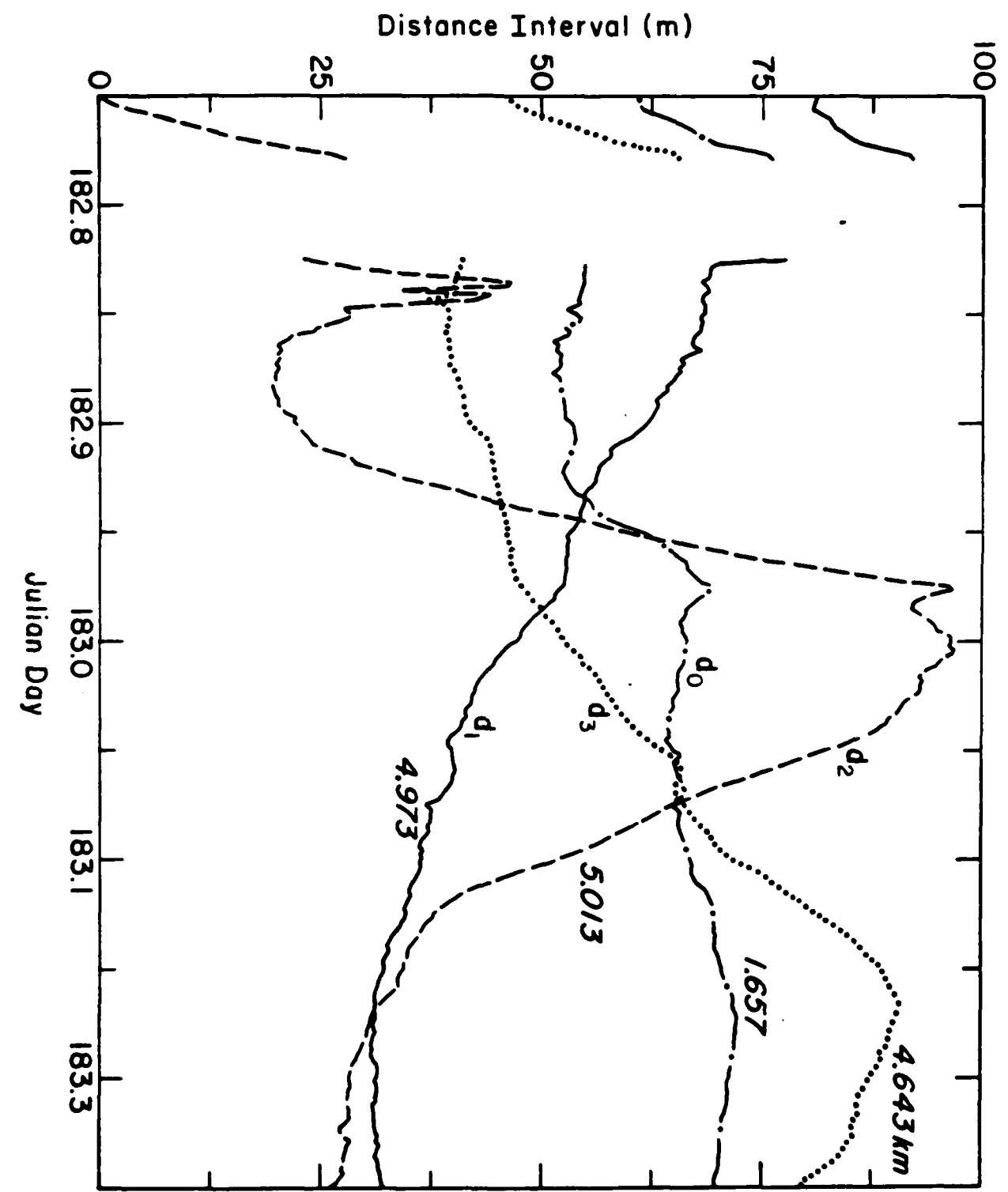


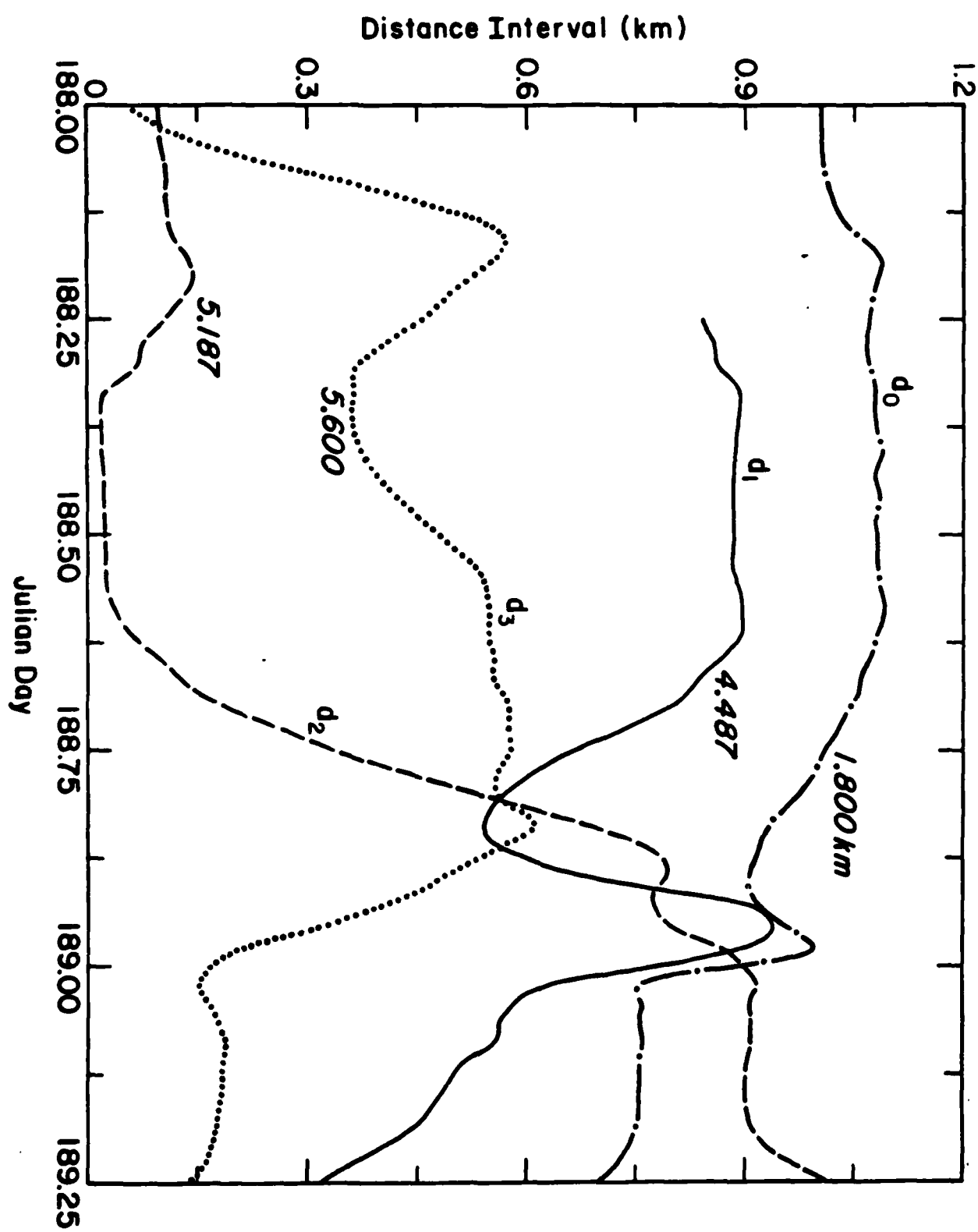
— 29 Jun (0800 GMT)
--- 2 Jul (0800 GMT)
- - - 8 Jul (0800 GMT)

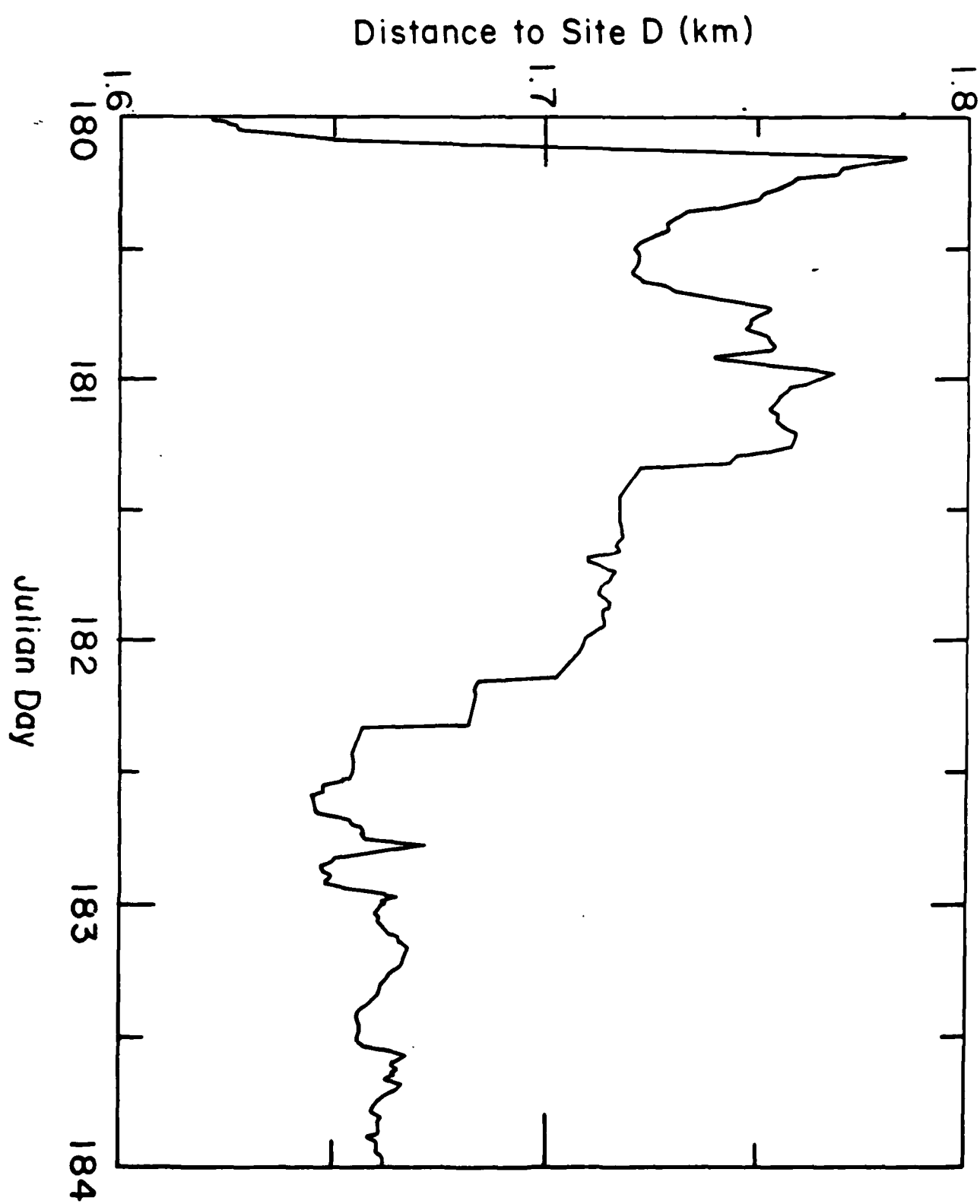


Open Water









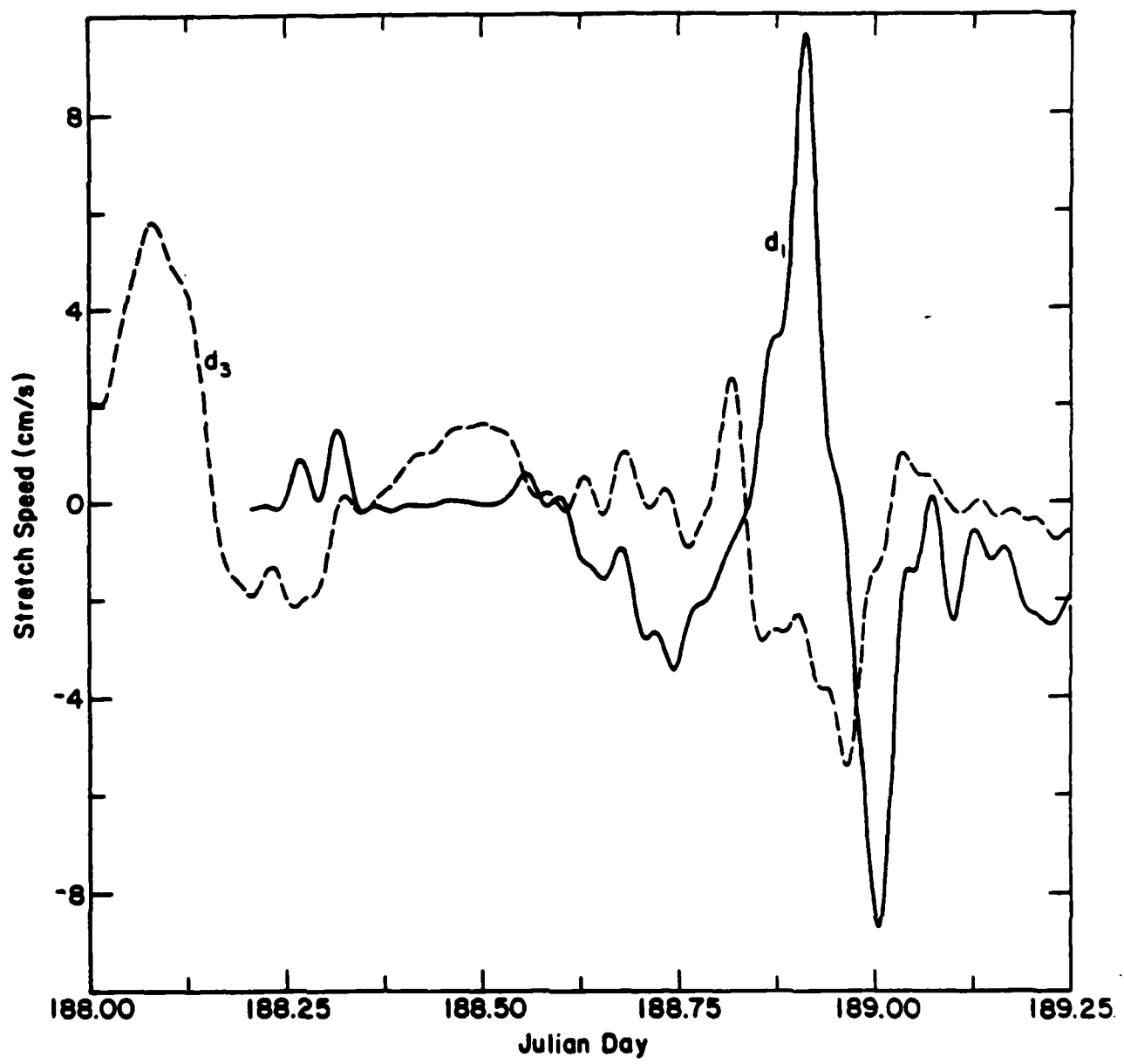
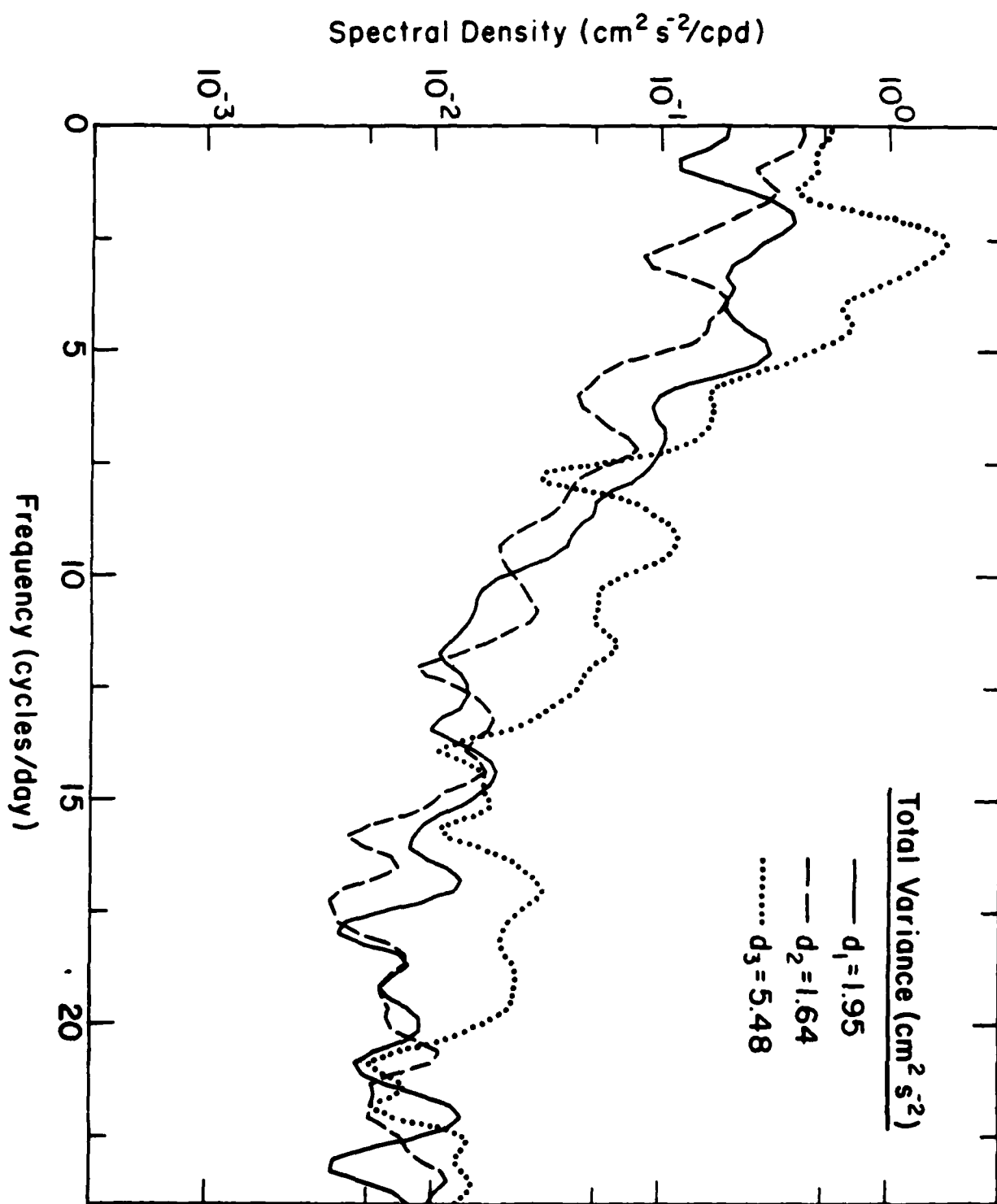
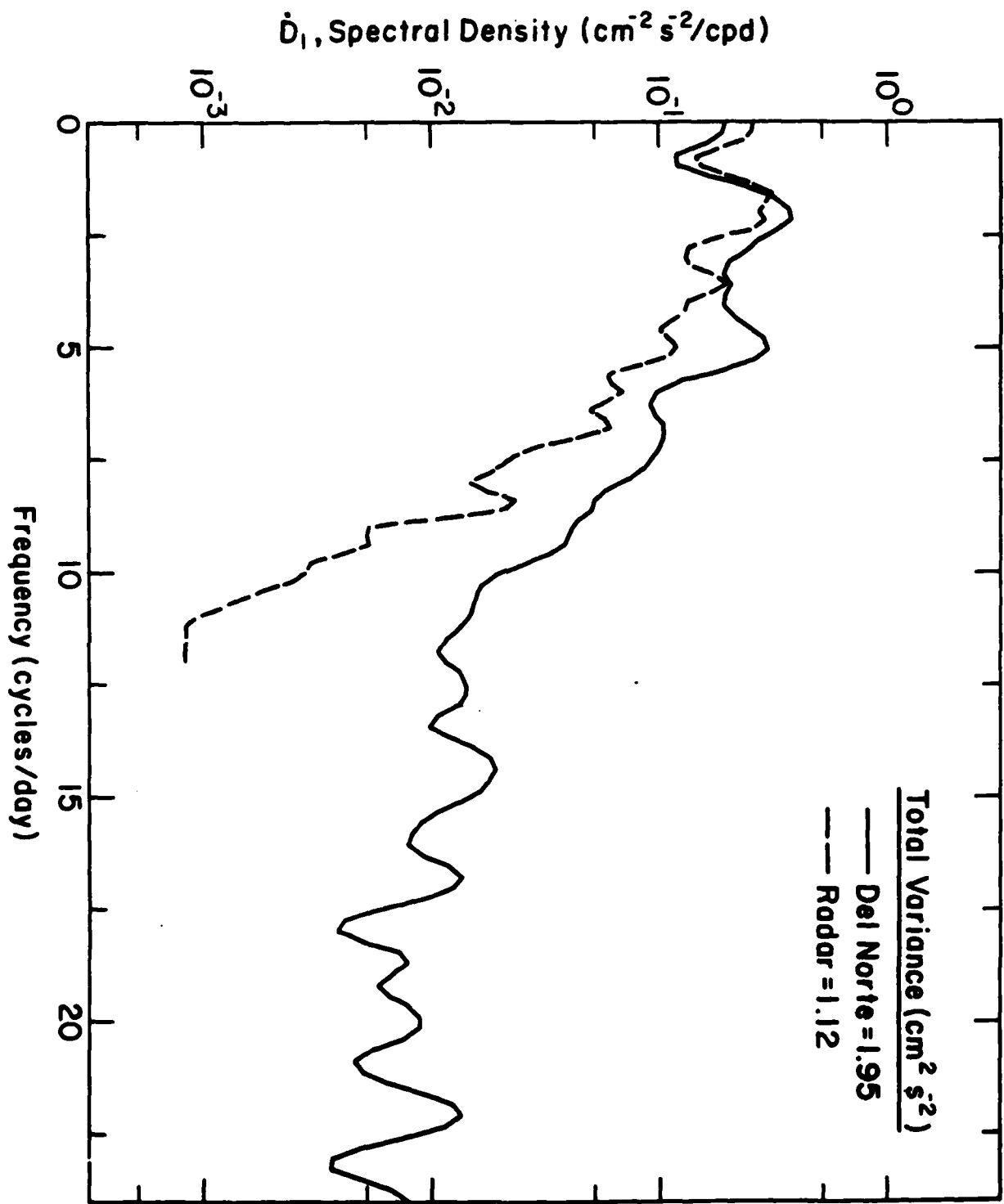


Fig 9





I : II

ANNEX

- a. The amount of unused funds: none
- b. Important property required: none

